

# A Fast Sensitivity-based Preventive Control Selection Method for Online Voltage Stability Assessment

Shuaihu Li, Yi Tan, Canbing Li, Yijia Cao, Lin Jiang

**Abstract**— Modern power system suffers voltage instability more frequently due to the increasing load. Sensitivity analysis based preventive control is widely recognized as an effective method for preventing voltage instability. However, the well-known load margin (LM) based sensitivity methods are not suitable for real-time application since they must solve the left eigenvector of zero eigenvalue of the Jacobi matrix at the critical point and require the system-wide information. Therefore, this paper proposes a fast sensitivity-based method for selecting the most effective preventive controls. The sensitivity analysis uses a local voltage stability index, i.e., load impedance modulus margin (LIMM) which is derived from the local measurements (nodal voltage and current), and the sensitivity ranking can be obtained more accurately and faster than traditional methods based on load margin. Such computational advantages make it suitable for online application. The effectiveness of the proposed method is successfully validated by both small and large-scale power systems.

**Keywords**— Voltage stability, preventive control, sensitivity analysis, load impedance module margin

## NOMENCLATURE

CPFLOW	Continuation power flow method
CPFSA	Sensitivity analysis based CPMFLOW
DG	Distributed generation
EVSI	External voltage stability index
FACTS	Flexible alternative current transmission system
FSA	Fast linearization sensitivity analysis method
HVDC	High voltage direct current
ISI	Impedance stability index
LIMM	Load impedance modulus margin
LIMM-SA	Sensitivity analysis method based on LIMM
LM	Load margin
LVSI	Line voltage stability index
MLP	Maximum loadability point

PMU	Phasor measurement unit
VSA	Voltage stability assessment
VSM	Voltage stability margin
SMARTDevice	Stability monitoring and reference tuning device

## I. INTRODUCTION

VOLTAGE stability assessment (VSA) has been developed to prevent voltage instability in presence of insufficient security margins of power systems. With the increasing load and enlarged interconnection of power grid, modern power system is more likely to be operated under a stressed state. In the past decades, serious blackouts related to voltage collapse occurred more frequently [1]-[3], requesting a more advanced VSA tool.

Preventive control is usually designed to take control actions to change the critical contingencies with the insufficient voltage stability margins (VSM) into non-critical ones as soon as possible, and is usually implemented in the control center for a global decision. Many methods have been developed for preventive control selection [6]-[16]. The optimization-based technique is one of these approaches to select the optimal control variables. In earlier research, most of the optimization models are designed to minimize the control cost with certain security constraints. However, they are impractical since many control variables must be taken account into the optimization model [8]. Therefore, alternative approaches have been developed to detect and discard less-effective control variables to enhance the computational speed [9]-[13]. In these methods, the sensitivities of VSM with respect to control variables are obtained by solving the left eigenvector of the zero eigenvalue of Jacobian matrix at the critical point. The critical point is often assessed by using CPMFLOW to obtain MLP, which requires available system-wide information [14]-[16]. Remarkable time is required by the calculation of eigenvector and MLP, especially for a large-scale power system. However, the operating state of modern power system is more likely to be changed by faults and the rapid-response devices such as HVDC, FACTS and distributed generation (DG) [17]. In this regard, the efficient and fast control selection method is needed for the real-time application.

To speed up the sensitivity analysis for VSA, an approach based on Look-Ahead method was proposed for calculating sensitivity of VSM with respect to control variable in [18]-[19]. In this method, LM is estimated by using the quadratic

This work was supported by the National Natural Science Foundation of China (NSFC) under Grant 51777179 and Engineering and Physical Sciences Research Council under Grant EP/L014351/1, and in part supported by the 111 Project of China. Corresponding author: Y. Tan.

S. Li is with the College of Information Engineering, Xiangtan University, Xiangtan 411105, China (e-mail: lishuaihu2010@126.com).

Y. Tan, C. Li, and Y. Cao are with the College of Electrical and Information Engineering, Hunan University, Changsha 410082, China (e-mail: yibirthday@126.com; licanbing@qq.com; yjcao@hnu.edu.cn).

L. Jiang is with the Faculty of Science and Engineering, School of Electrical Engineering, Electronics and Computer Science, the University of Liverpool, Liverpool L69 3GJ, UK. (e-mail: L.Jiang@liverpool.ac.uk).

approximation of the PV curve. The sensitivity of LM with respect to control variable is calculated without computing MLP via CPFLOW. The speed of preventive control selection is improved obviously, but the maximum loading of the transmission system is fixed which depends on the network topology, generation and load patterns and the availability of VAR resources, therefore, the estimation error of LM by using the quadratic approximation of the PV curve is inevitable. This can cause the error of sensitivity calculation, limiting the application of the method in [18]-[19]. As the technology advances, several local voltage stability indexes have been proposed to realize online voltage stability monitoring, such as LVSI, ISI and EVSI [20]-[25] etc. Those local indexes can be calculated in the SMARTDevice [22] by using sole local information to track the distance to voltage instability. SMARTDevice can send the result of local index to the control center for a global decision. In the multi-level hierarchy voltage control architecture, the upper-level control normally takes precedence over local devices. SMARTDevices can carry out their own decisions to mitigate the aggravating situation in case of emergency such as communication channels failing. The decision is often made by comparing the current local index against a fixed threshold. However, it is difficult to accurately choose the fixed threshold in practical and thus a conservative value is often used which could result in unnecessary load shedding. Moreover, the quantity of load shedding that contributes to improve voltage stability cannot be easily obtained, and there is a lack of research on direct local indicator to measure the control effect on improving VSM.

In this context, this paper selects the local index LIMM proposed in [26] as VSM for preventive control selection. This index can evaluate voltage stability more exactly and faster based on the local measurements (nodal voltage and current), and the Thevenin impedance and load impedance used to calculate LIMM are obtained by a relatively simple expression. On basis of that, a fast sensitivity analysis method based on LIMM (called LIMM-SA) is proposed to select the most effective preventive control variable which assists the control center to make a global protection decision.

The main contributions of this paper can be summarized as follows:

1) Using the current common methods, the system-wide information is required for calculating sensitivities of controls with respect to LM. In contrast, the local index, LIMM, is used to evaluate the sensitivity of a preventive control variable with respect to VSM in our paper, and it can be implemented in the SMARTDevice based on the local measurements. The elapse time is much smaller than the traditional methods, since there is no need of the calculation of the critical point via CPFLOW and the left eigenvectors of zero eigenvalue of the Jacobi matrix at the critical point;

2) The sensitivities are collected by the control center for selecting the most effective control variable. Considering the limits of the selected control variable, the optimal selection can be implemented by optimizing the preventive control scheme in a more efficient way.

3) Simulation results successfully validate that the proposed method is much faster and has a good accuracy as compared with the well-known load margin (LM) based sensitivity methods.

The rest of this paper is organized as follows. Section II gives a short introduction on LIMM. Section III presents the LIMM-SA method for VSA. This proposed method is tested on three systems in Section IV, i.e., the IEEE 39-Bus system, a reduced model of Guangdong power system, China southern power grid. Section V summaries the main conclusions of the proposed LIMM-SA method.

## II. LOAD IMPEDANCE MODULUS MARGIN

LIMM is a local index for assessing voltage stability margin, which was derived from Thevenin equivalent method. It can be derived as follows.

First, consider the condition of the power systems reaching maximum transmission power below:

$$|Z_{iLD}| = |Z_{iTHEV}| \quad (1)$$

where  $|Z_{iLD}|$  and  $|Z_{iTHEV}|$  are the load equivalent impedance and the system equivalent impedance at the  $i$ th node, respectively. They can be calculated by:

$$Z_{iLD} = \frac{\dot{V}_i}{\dot{I}_i} \quad (2)$$

$$Z_{iTHEV} = \frac{d\dot{V}_i}{d\dot{I}_i} = \frac{d\dot{V}_i/d\lambda}{d\dot{I}_i/d\lambda} \quad (3)$$

where  $\dot{V}_i$ ,  $\dot{I}_i$  is the  $i$ th nodal voltage and current, respectively;

$\lambda$  is an intermediate variable to obtain  $Z_{iTHEV}$  [26], because the derivative of bus voltage with respect to load current cannot be calculated directly in a complex domain due to the non-analytic property of power system.

Then, the load impedance modulus margin ( $\eta_i$ ) can be defined as follows:

$$\eta_i = \frac{|Z_{iLD}| - |Z_{iTHEV}|}{|Z_{iLD}|} \quad (4)$$

According to the simple expression of the (2) and (3),  $\eta_i$  can be obtained directly with known nodal voltage and current from PMU. The value of the LIMM ranges from 0 to 1, and  $\eta_i=0$  represents the critical point where Thevenin impedance is equal to load impedance. For practical usage, the LIMM of the pilot node owing the minimum value of  $\eta_i$  under the base case is used to indicate the VSM [22]. The effectiveness of LIMM for voltage stability evaluation have been successfully verified in [26]. In the realistic environment, measurements are not precise and the Thevenin parameters drift due to the system's changing states [27]-[28]. To suppress oscillations, a larger data window needs to be used. The filtering method in [29] is used in this study, which is to smooth all signals before calculating sensitivities to address practical issues such as data memory, window size, noise in measurements, close-by faults, and so on.

## III. LIMM-BASED SENSITIVITY ANALYSIS

Sensitivity analysis is to measure the variation of VSM with respect to control variable. This section is to demonstrate the LIMM based sensitivity analysis method in which first-order

derivative based sensitivity analysis is carried out first and then the second-order derivative is used to further revise results obtained by first-order derivative based sensitivity analysis.

#### A. First-order derivatives

In general, the power flow equations can be formulated by:

$$F(\mu_j, \lambda, \dot{V}) = 0 \quad (5)$$

where  $\lambda$  is the load parameter, which reflects the real-time load variation direction;  $\dot{V}$  is the voltage vector;  $\mu_j$  is the  $j$ th control variable. Load variation and control variable are the disturbances should be considered in sensitivity analysis.

Linearizing (5), the following equation can be obtained:

$$F_\lambda \Delta \lambda + F_{\dot{V}} \Delta \dot{V} + F_{\mu_j} \Delta \mu_j = 0 \quad (6)$$

Assume  $\lambda$  is constant at the current operating point, so load is constant and the system has only one disturbance (i.e. control variable). Thereby, the (6) can be simplified as follows:

$$\frac{\partial F}{\partial \dot{V}} \Delta \dot{V} + \frac{\partial F}{\partial \mu_j} \Delta \mu_j = 0 \quad (7)$$

where  $\partial F / \partial \dot{V}$  equals to Jacobian Matrix of the base case.  $\partial F / \partial \mu_j$  is known, thus the approximation of  $\Delta \dot{V} / \Delta \mu_j$  is obtained by:

$$\frac{\Delta \dot{V}}{\Delta \mu_j} = - \left( \frac{\partial F}{\partial \dot{V}} \right)^{-1} \cdot \frac{\partial F}{\partial \mu_j} \quad (8)$$

The nodal current  $\dot{I}_i$  can be obtained by:

$$\dot{I}_i = \frac{\hat{S}_i}{\hat{V}_i} \quad (9)$$

where  $S_i$  is the apparent power of the  $i$ th node and  $\dot{V}_i$  is obtained by PMU; the hat “Λ” on top denotes the conjugate complex.

Differentiating (9) with respect to the control variable  $\mu_j$ , the first-order derivative  $d\dot{I}_i / d\mu_j$  can be determined by:

$$\frac{d\dot{I}_i}{d\mu_j} = \frac{\frac{d\hat{S}_i}{d\mu_j} - \dot{I}_i \frac{d\hat{V}_i}{d\mu_j}}{\hat{V}_i} \quad (10)$$

In order to determine  $d\dot{I}_i / d\mu_j$ , we get  $Z_{iLD}$  firstly by:

$$Z_{iLD} = V_i^2 / \hat{S}_i \quad (11)$$

Then,  $d\hat{S}_i / d\mu_j$  is calculated by:

$$\frac{d\hat{S}_i}{d\mu_j} = 2 \frac{V_i}{Z_{iLD}} \cdot \frac{dV_i}{d\mu_j} \quad (12)$$

Substituting the value obtained by (8), (11) and (12) into (10),  $d\dot{I}_i / d\mu_j$  is calculated.

From the above analysis, under the assumption of the constant load, we can get the (8) and (10) and then inserted them into (3) to obtain the 1st order derivative. That means

Thevenin impedance is determined. Thereby, L IMM can be obtained by (4) under the disturbance of  $\mu_j$ .

#### B. Second-order derivatives

In practical, a load is time-varying. Thus, except control variable, load parameter should be considered when analyzing the control sensitivity. To consider the impact of time-varying load parameter, the second-order partial derivatives of nodal voltage and current with respect to control variable and load parameter should be determined simultaneously.

Fixing the control variable  $\mu_j$  in (6), we can obtain:

$$\frac{\partial F}{\partial \lambda} + \frac{\partial F}{\partial \dot{V}} \frac{\Delta \dot{V}}{\Delta \lambda} = 0 \quad (13)$$

In (13),  $\partial F / \partial \lambda$  is known when the direction of load change is given. Hence, the approximation of  $\Delta \dot{V} / \Delta \lambda$  is obtained. Then, differentiating (13) with respect to the control variable  $\mu_j$ , the following equation can be obtained as follows:

$$\frac{\partial F}{\partial \dot{V}} \frac{\partial^2 \dot{V}}{\partial \lambda \partial \mu_j} = - \frac{\partial^2 F}{\partial \dot{V} \partial \mu_j} \frac{\Delta \dot{V}}{\Delta \lambda} - \frac{\partial^2 F}{\partial \mu_j \partial \lambda} \quad (14)$$

Solving the (14), the value of  $\frac{\partial^2 \dot{V}}{\partial \lambda \partial \mu_j}$  can be obtained [18].

Based on (11), the first-order derivative  $d\dot{I}_i / d\lambda$  can be obtained by:

$$\frac{d\dot{I}_i}{d\lambda} = \frac{\frac{d\hat{S}_i}{d\lambda} - \dot{I}_i \frac{d\hat{V}_i}{d\lambda}}{\hat{V}_i} \quad (15)$$

Then, differentiating (15) with respected to  $\mu_j$ , one can get:

$$\frac{\partial^2 \dot{I}_i}{\partial \lambda \partial \mu_j} = \frac{\frac{\partial^2 \hat{S}_i}{\partial \lambda \partial \mu_j} - \frac{d\dot{I}_i}{d\mu_j} \frac{d\hat{V}_i}{d\lambda} - \dot{I}_i \frac{\partial^2 \hat{V}_i}{\partial \lambda \partial \mu_j}}{\hat{V}_i} - \frac{\left( \frac{d\hat{S}_i}{d\lambda} - \dot{I}_i \frac{d\hat{V}_i}{d\lambda} \right) \frac{d\hat{V}_i}{d\mu_j}}{\hat{V}_i^2} \quad (16)$$

where  $d\dot{I}_i / d\mu_j$  and  $\frac{\partial^2 \hat{V}_i}{\partial \lambda \partial \mu_j}$  are obtained by (12) and (14) respectively.

#### C. L IMM based Sensitivity Analysis

Further, differentiating (3) with respect to the control variable  $\mu_j$ , the derivative of Thevenin impedance with respect to control variables  $\mu_j$  is obtained by:

$$\frac{dZ_{iTHEV}}{d\mu_j} = \frac{d \left( \frac{d\dot{V}_i / d\lambda}{d\dot{I}_i / d\lambda} \right)}{d\mu_j} \quad (17)$$

which can be expanded by:

$$\frac{dZ_{iTHEV}}{d\mu_j} = \frac{\frac{\partial^2 \dot{V}_i}{\partial \lambda \partial \mu_j} \frac{d\dot{I}_i}{d\lambda} - \frac{\partial^2 \dot{I}_i}{\partial \lambda \partial \mu_j} \frac{d\dot{V}_i}{d\lambda}}{\left(\frac{d\dot{I}_i}{d\lambda}\right)^2} \quad (18)$$

Inserting (13) (14), (15) and (16) into (18),  $dZ_{iTHEV}/d\mu_j$  is obtained. Similarly, the derivative of the load equivalent impedance with respect to control variable is obtained by:

$$\frac{dZ_{iLD}}{d\mu_j} = \frac{d\left(\frac{\dot{V}_i}{\dot{I}_i}\right)}{d\mu_j} = \frac{\frac{d\dot{V}_i}{d\mu_j} \dot{I}_i - \frac{d\dot{I}_i}{d\mu_j} \dot{V}_i}{I_i^2} \quad (19)$$

where  $d\dot{V}_i/d\mu_j$  and  $d\dot{I}_i/d\mu_j$  are calculated via (10) and (12), respectively.

Based on (18) and (19), we can get:

$$\begin{cases} \Delta Z_{iTHEV} = \frac{dZ_{iTHEV}}{d\mu_j} \cdot \mu_j \\ \Delta Z_{iLD} = \frac{dZ_{iLD}}{d\mu_j} \cdot \mu_j \end{cases} \quad (20)$$

Then, the value of post-control L IMM,  $\eta'_i$ , is obtained by

$$\eta'_i = \frac{|Z_{iLD0} + \Delta Z_{iLD}| - |Z_{iTHEV0} + \Delta Z_{iTHEV}|}{|Z_{iLD0} + \Delta Z_{iLD}|} \quad (21)$$

For a large-scale power system, it is impractical to calculate the variation of all nodal VSM for each control variable. In [20], the pilot node is defined to assess VSM of power system, which has the minimum value of L IMM. Thus, at the current operating point, VSM is determined by the L IMM of the pilot node, which is denoted by  $\rho_0$  as:

$$\rho_0 = \min(\eta_i) \quad (22)$$

And the variation of VSM of the pilot node is:

$$\Delta \rho = \rho - \rho_0 \quad (23)$$

where  $\rho = \eta'_i$  and  $\Delta \rho$  is VSM and the variation of VSM considering the disturbances of load variation and control variable, respectively.

The sensitivity of VSM with respect to  $\mu_j$  can be obtained by:

$$S_j = \frac{\Delta \rho}{\Delta \mu_j} \quad (24)$$

#### D. Calculation Procedure of L IMM-SA

As shown in Fig.1, given  $N_c$  as the number of the control variables, the main steps for the proposed L IMM-SA and ranking the control variables are summarized as follows:

1) Initialize  $c=0$ . Let  $S$  and  $\Gamma$  be the sets of sensitivities of the preventive control variables and the critical contingencies, respectively. Initialize  $\Gamma = \{ \}$   $S = \{ \}$  as a null set;

2) The original data collected from PMU is subtracted by

the filtering method according to [29].

3) According to (4), for a post-contingency case, the L IMM  $\eta_i$  is calculated under a specific direction of load increase. Let the  $i$ th node be the pilot node owning the minimum L IMM.

4) Judge if  $0 \leq \eta_i^{c_k} \leq \eta_{threshold}$  (the threshold is determined by the system operator according to the operating experience). If so, the corresponding contingencies  $C_k$  is incorporated in the critical contingency set  $\Gamma$ . Otherwise, it is incorporated in the contingency set which are protected by emergency control or economical schedule.

5) Under the post-contingency case, select  $\mu_j$  randomly within its upper and lower limits ( $\mu_j^{\min} \leq \mu_j \leq \mu_j^{\max}$ ), which represent reactive power limit of generator, available taps of OLTC, etc.; Calculate the first-order derivatives based on (8) and (10) to obtain  $d\dot{V}_i/d\mu_j$  and  $d\dot{I}_i/d\mu_j$ ; Calculate  $dZ_{iTHEV}/d\mu_j$  and  $dZ_{iLD}/d\mu_j$  via (18) and (19);

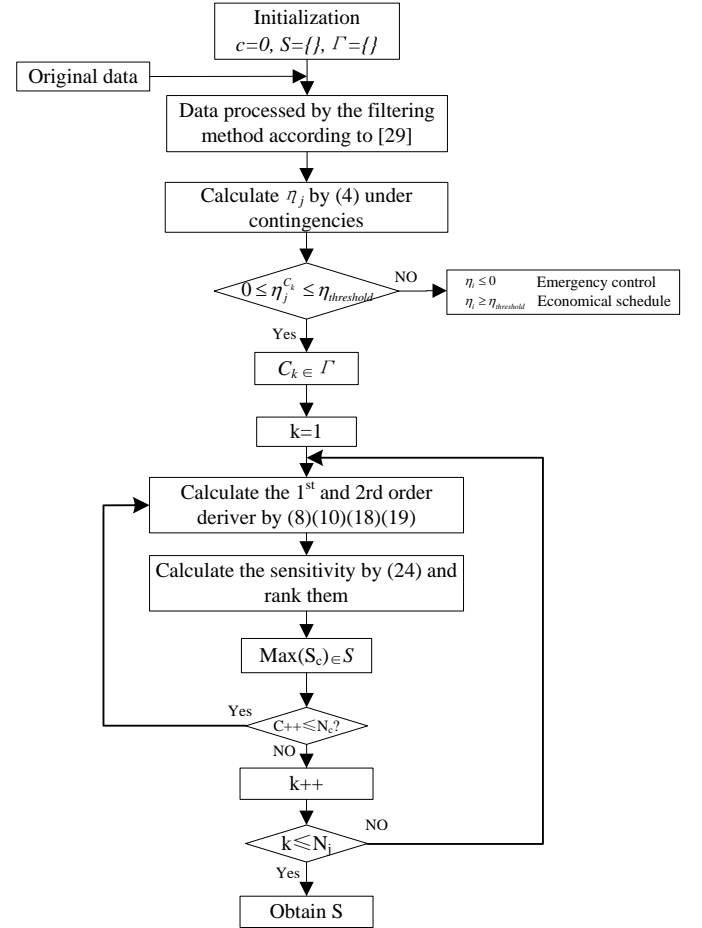


Fig.1 Flowchart of the proposed method for preventive control selection

6) Calculate the second-order derivatives  $\frac{\partial^2 \dot{V}}{\partial \lambda \partial \mu_j}$  and  $\frac{\partial^2 \dot{I}_i}{\partial \lambda \partial \mu_j}$  based on (14) and (16);

7) Calculate  $\eta'_i$  via (21) and the sensitivity  $S_j$  via (24), and obtain  $S = S \cup \{S_j\}$  (i.e., insert the sensitivity  $S_j$  into the

set  $S$ );

8)  $c = c + 1$ , If  $c$  is less than or equal to the available number of control variables  $N_c$ , then go to step 3;

9) Rank the elements of  $S$  for the control variables in decreasing order, and finally the most effective control variables can be selected.

Note that practical control variables are often divided into three types according to their control costs. Type 1 consists of generator terminal voltage, shunt capacitor, and transformer tap adjustment; type 2 is generator output power; type 3 is load curtailment. From the perspective of the grid operator, the control effectiveness is not only the decision factor in existing preventive control selection methods, and most of them need to consider control cost in optimization objective [19]. This work focuses on the selection of the most effective preventive control variables. To satisfy the application, the rankings of different types of control variables can be obtained in term of the proposed sensitivities. Based on this rank, these control variables of small sensitivities are eliminated. Therefore, only those effective variables are considered in the optimization space, and the efficiency of control selection will be greatly improved.

#### IV. CASE STUDY

In this section, time domain simulations are conducted on the IEEE 39-bus system [30], a reduced model of Guangdong power system and a large-scale power system of China southern power grid to simulate the real-time data collected from PMU. The simulations are run on a personal computer with 8 GB of RAM. The software PSD-BPA (power system integrated simulation software) is adopted to get the system operating data and thus no measurement error is considered. Then, the programs of LIMM-SA, LASA and FSA algorithms are run in the MATLAB. The sensitivities obtained by LIMM-SA are compared with results of LASA method [13], fast linearization sensitivity analysis method (FSA) [18], and sensitivity analysis based CPFLOW (CPFSA) [15] to validate the effectiveness of the proposed method in selecting the most effective preventive control variables.

##### A. Case 1: IEEE 39-Bus system

The IEEE 39-bus system consists of 10 generators and 19 load nodes. The constant active power load model is used and the number of loads is uniformly increased to be 1.05 times of the initial value at 0.1 s (i.e.  $\lambda=1.05$ ). The bus 31 is selected as the swing bus and does not participate in control. The increased active and reactive loads are shared according to the initial power ratio between the power generators, and the network loss changes are consumed by the swing bus, and the limit of reactive power limit of PV node is considered, i.e., the PV node will be converted into a PQ node if the reactive generation exceeds the limit. For simplicity, only other nine generators are used as control variables in this case. The control variables are constrained by their upper and lower boundaries, so these variables are always in the available regions.

To simulate a stressed operating state, the system load is modified to be 1.55 times of its initial operation condition given in [30]. Under the modified case, the contingencies were scanned and classified via LIMM and the critical ones are

selected according to the guidelines of the minimum VSM provided by the control center [18]. In this case, a minimum VSM of 10% must be ensured with consideration of real-time operation. Thereby, the result of the critical contingency analysis is listed in Table I.

TABLE I  
CRITICAL CONTINGENCY ANALYSIS

Fault ID	Fault # (outage of the line)	VSM	
		The minimum LIMM obtained by LIMM-SA (p.u.)	LM by CPFSA (p.u.)
Normal	No	0.2605	0.2002
C1	17-18	0.0809	0.0881
C2	3-18	0.0468	0.0443

As shown in Table I, the difference between the results of LIMM and LM are small. The values of the minimum LIMM in the third column represent the real voltage stability levels of power system under various cases. The same critical contingencies are selected by the two VSMs, which verifies the accuracy of LIMM in VSA.

##### 1) Sensitivity Analysis

The proposed algorithm is applied to calculate sensitivities of VSM with respect to control variables. The ranked sensitivities of LIMM-SA, LASA, and CPFSA for those 2 critical contingencies are presented in Table II and Table III, respectively. The rankings are obtained according to the sensitivities of control variables. The order is represented with numbers in parentheses.

TABLE II  
RANKED SENSITIVITY ANALYSIS RESULTS OF LIMM-SA FOR THE OUTAGE  
LINE (17–18)

Control	Sensitivity			
	CPFSA	LASA	FSA	LIMM-SA
G38_P	0.00933(1)	0.00928(1)	0.00913(1)	0.00926(1)
G36_P	0.00905(2)	0.00904(2)	0.00902(2)	0.00903(2)
G37_P	0.00886(3)	0.00855(3)	0.00822(3)	0.00869(3)
G33_P	0.00875(4)	0.00831(4)	0.00796(4)	0.00854(4)
G32_P	0.00799(5)	0.00776(5)	0.00733(5)	0.00782(5)
G34_P	0.00746(6)	0.00728(6)	0.00702(6)	0.00733(6)

TABLE III  
RANKED SENSITIVITY ANALYSIS RESULTS OF LIMM-SA FOR THE OUTAGE  
LINE (3–18)

Control	Sensitivity			
	CPFSA	LASA	FSA	LIMM-SA
G37_P	0.00806(1)	0.00865(1)	0.00849(1)	0.00825(1)
G39_P	0.00769(2)	0.00819(2)	0.00802(2)	0.00799(2)
G35_P	0.00622(3)	0.00626(4)	0.00614(4)	0.00623(3)
G34_P	0.00586(4)	0.00634(3)	0.00631(3)	0.00607(4)
G32_P	0.00512(5)	0.00532(5)	0.00520(5)	0.00517(5)
G33_P	0.00463(6)	0.00443(6)	0.00419(6)	0.00484(6)

Results in Tables II show that the LIMM-SA can obtain the same rankings as the CPFSA, FSA and the LASA. Observing Table III, for the LASA and FSA method, there is an exchange between the 3th and 4th most effective control variables for C2 contingency, as compared with LIMM-SA and CPFSA. Therefore, taking CPFSA as the reference, it is found that the sensitivity ranking obtained by LIMM-SA coincides with CPFSA for the above two critical contingencies, and thus LIMM-SA is more accurate than LASA and FSA. Moreover, as shown in Table I, the system state is closer to the critical point

under C2 contingency than C1. So, we can deduce that the sensitivity ranking obtained by LIMM-SA is more accurate than LASA and FSA when it is close to the critical point. The main reason is that the linearization and approximation of LASA and FSA enlarge the error of VSM evolutions when the power system is operated in the neighborhood of MLP.

## 2) Sensitivity results obtained by 1st-and 2rd-order

To demonstrate the effectiveness of the proposed LIMM-SA method in the case of load variation, the first-order (1st-order) derivative based LIMM-SA method (Section III-A) and the proposed second-order (2<sup>rd</sup>-order) derivative based LIMM-SA (Section III-B) are compared in Fig.2, and the sensitivities calculated by CPFSA are used as the reference.

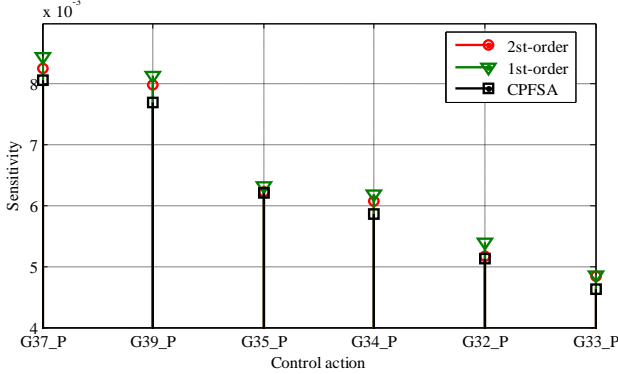


Fig.2 The comparison chart of sensitivity analysis for the outage of line 3-18

Results in Fig.2 show that the proposed 2rd-order LIMM-SA can greatly improve the calculation accuracy than the 1<sup>st</sup>-order LIMM. The average error between the 1<sup>st</sup>-order LIMM and the CPFSA is 4.77% while the average error between the 2rd-order LIMM and the CPFSA is 2.58%. This indicates an improved accuracy around 45% in this case.

## B. Case 2: 273-bus Guangdong province power system

In this section, a larger real-world power system, i.e., a reduced model of Guangdong power system, is used to verify the effectiveness of the proposed LIMM-SA method. As shown in Table IV, there are 51 generators, 190 loads, 236 shunt capacitors, 58 tap changer transformers, 6 synchronous compensators, which can be used as control units. The model of loads and their time-varying feature are the same as Case 1.

TABLE IV

THE INFORMATION OF 273-BUS GUANGDONG PROVINCE POWER SYSTEM

Basic situation		Available for voltage control	
Name	number	Control#	number
Buses	273	Generator rescheduling	51
Generators	97	tap changer transformers	58
capacitor	263	synchronous compensator	6
lines	368	shunt capacitors	236
loads	190	Load curtailment	190

In the critical contingency, its feature is defined that the VSM is less than 10% in the post-contingency state. In the initial state, the VSMs of all N-1 contingencies are larger than 10%, hence there are no critical contingency. During the N-2 contingencies test, as shown in Table V, LIMM values are all less than 10% in all post-contingencies.

Table V shows that LIMM-SA obtains the same rankings and the critical contingency set as CPFSA, which verifies the accuracy of LIMM again. As is well known, power system shows more intense nonlinear characteristic when the operating

point is close to MLP. Therefore, errors in these methods based on linearization (LASA, FSA) would be more likely to become larger. The LIMM of the system is 0.0983 under the critical contingency C1055, which is a little smaller than 0.1. And the LIMM is 0.0136 under the C1132, which is closer to the critical point than the C1055.

TABLE V  
CONTINGENCY ANALYSIS RESULT

Fault ID	VSM	
	The minimum LIMM by LIMM-SA (p.u.)	LM by CPFSA (p.u.)
No fault	0.3236	0.1961
C1132	0.0136	0.0153
C1155	0.0156	0.0180
C0609	0.0365	0.0331
C0962	0.0568	0.0540
C1055	0.0983	0.0962

Table VI and VII present the results of sensitivity ranking analysis obtained by LIMM-SA, LASA, FSA and CPFSA under C1055 and C1032, respectively, in which rescheduling generators' power outputs is taken as control object. From the second, fifth columns of Table VI and Table VII, the sequence obtained by LIMM-SA always coincides with the sequence obtained by CPFSA under the two contingencies. But there are some differences in LASA and FSA, e.g., the 6<sup>th</sup> and 7<sup>th</sup> control variables in Table VI. Moreover, under the contingency C1032, the results show the difference between the values obtained by CPFSA and LIMM-SA is the smallest. That reveals the control rankings determined by LIMM-SA is more robust and accurate, especially when it is operated near MLP.

TABLE VI

RANKED SENSITIVITY ANALYSIS RESULTS OF LIMM-SA FOR THE C1055

Control	Sensitivity			
	CPFSA	LASA	FSA	LIMM-SA
G36_P	0.00806(1)	0.00812(1)	0.00290(1)	0.00825(1)
G19_P	0.00769(2)	0.00786(2)	0.00794(2)	0.00789(2)
G25_P	0.00622(3)	0.00632(3)	0.00639(3)	0.00623(3)
G47_P	0.00586(4)	0.00596(4)	0.00608(4)	0.00607(4)
G26_P	0.00512(5)	0.00521(5)	0.00532(5)	0.00517(5)
G35_P	0.00463(6)	0.00455(7)	0.00449(7)	0.00484(6)
G50_P	0.00452(7)	0.00461(6)	0.00468(6)	0.00471(7)
G40_P	0.00406(8)	0.00411(8)	0.00424(8)	0.00407(8)
G06_P	0.00399(9)	0.00389(9)	0.00405(9)	0.00372(9)
G13_P	0.00385(10)	0.00377(10)	0.00368(10)	0.00376(10)

The transformer tap change is another kind of commonly used voltage regulation measures. The sequence obtained by the LIMM-based sensitivity method for the three steps of the transformer tap change control is presented in Table VIII.

Table VIII shows that the ranked results for the three control steps are also the same as CPFSA. The results indicate the robustness of the LIMM-Based sensitivity under the different control steps. Besides, Table VII-VIII validate that the LIMM-SA method is effective in adjusting transformer tap changer and generator rescheduling. This indicates that LIMM-SA could also be extended for other control variables, such as shunt capacitor, static VAR compensators etc.

TABLE VII

RANKED SENSITIVITY ANALYSIS RESULTS OF LIMM-SA FOR THE C1132

Control	Sensitivity
---------	-------------

	CPFSA	LASA	FSA	LIMM-SA
G22_P	0.005648(1)	0.005332(1)	0.006823(1)	0.005004(1)
G06_P	0.005235(2)	0.005012(2)	0.005744(2)	0.004633(2)
G35_P	0.003616(3)	0.003616(3)	0.003916(4)	0.003168(3)
G07_P	0.003222(4)	0.003222(4)	0.004222(3)	0.002808(4)
G33_P	0.002404(5)	0.002404(5)	0.002404(5)	0.002062(5)
G18_P	0.001865(6)	0.001865(6)	0.001865(6)	0.001571(6)
G09_P	0.001199(7)	0.001299(8)	0.001599(8)	0.000969(7)
G12_P	0.001028(8)	0.001328(7)	0.001928(7)	0.000801(8)
G41_P	0.000531(9)	0.000466(9)	0.000988(9)	0.000464(9)
G44_P	0.000176(10)	0.000287(10)	0.000688(10)	0.00015(10)

TABLE VIII

RANKED SENSITIVITY ANALYSIS RESULTS OF LIMM-SA FOR THE C1055

Control	CPFSA	LIMM-Based Sensitivity		
		1 <sup>st</sup> step	2 <sup>nd</sup> step	3 <sup>rd</sup> step
T12	0.00411(1)	0.00409(1)	0.00408(1)	0.00412(1)
T40	0.00397(2)	0.00395(2)	0.00393(2)	0.00403(2)
T11	0.00387(3)	0.00384(3)	0.00382(3)	0.00397(3)
T15	0.00317(4)	0.00303(4)	0.00301(4)	0.00313(4)
T13	0.00261(5)	0.00258(5)	0.00256(5)	0.00260(5)
T29	0.00155(6)	0.00153(6)	0.00154(6)	0.00163(6)
T52	0.00133(7)	0.00130(7)	0.00131(7)	0.00134(7)
T21	0.00118(8)	0.00115(8)	0.00113(8)	0.00115(8)
T26	0.00085(9)	0.00083(9)	0.00082(9)	0.00089(9)

### C. Comparison of Calculation Speed

#### 1) Time Analysis of Case 2

At first, the calculation time of the main steps of the different methods are analyzed for Case 2, including contingencies screening time and sensitivity analysis time. The results are listed in Table IX., which shows, comparing with LASA, the contingency screening time is greatly reduced by the proposed method, using only 38% of LASA. For one contingency, LIMM calculation time includes the fixed 0.1s for sampling and average 0.02s for solving the system differential-algebraic equations (DAEs). LM calculation time needs about 0.31s on average due to multiple iterations to solve power flow equations. Therefore, for all 125 preconceived contingencies, the total time (15s) of LIMM-SA is far less than that of LASA (39s), as shown in Table IX.

TABLE IX

COMPARING THE CALCULATION TIME BY USE OF THREE METHODS IN CASE 2

Calculation Step	Calculation time (s)			Reduced Percentage
	LASA	FSA	LIMM-SA	
Contingency screening	39	16	15	38%/6.3%*
Sensitivity analysis	24	15	14	45%/6.7%
Total	63	31	29	41%/6.5%

\*This is obtained by  $38\% = \frac{(39-15)}{39}$  and  $6.3\% = \frac{(16-15)}{16}$ , and the following values are obtained in similar expressions.

The sensitivity analysis time of LIMM-SA is reduced by 45% as compared with LASA. The main reason is that LASA needs to solve the left eigenvectors of eigenvalues zero of the Jacobi matrix at the critical point. This process consumes more time than solving DAEs proposed in LIMM-SA. FSA is also a fast method, which only need two power flow solutions and

then solve the corresponding DAEs to achieve sensitivities, so the time is very close to LIMM-SA. The total time of LIMM-SA is still reduced by 6.5% as compared with FSA. Therefore, it is obvious the proposed method greatly reduces the contingency screening time, using only 38% of LASA.

#### 2) Time analysis on a large-scale realistic power system

In this section, we further compare the calculation time of different methods in a large-scale realistic power system, i.e., China southern power grid. This system has 5713 nodes, 6635 lines, and 642 adjustable points and is a much larger system than previous systems.

TABLE X  
COMPARING THE CALCULATION TIMES OF THREE CASES

Case	Calculation time (s)		
	LASA	FSA	LIMM-SA
Case 3: China southern power grid	295	182	79

As shown in Table X, the calculation time in this case by LIMM-SA is much less than the time of FSA. The LIMM-SA takes 79 seconds, and FSA took 182 seconds. Therefore, LIMM-SA saved more than half of the computation time. Also, from Tables IX-X, one can see that the larger the system size is, the more the saving running time is.

### V. CONCLUSION

In this paper, a fast sensitivity analysis method for VSM with respect to control variables is proposed in the context of local voltage stability index LIMM. In this method, the sensitivity of the dynamic impedance and the load impedance of LIMM on control variables is computed via the first-and second-derivative of nodal voltage and current with respect to control variables based on the local measurements. Then, the sensitivity of the control variables with respect to LIMM is obtained, which assists the control center to make a global protection scheme. The simulation results of the three different-scale cases show that sensitivity rankings computed by the proposed method are closer to the results obtained by CPFSA than LASA and FSA when system is operated in the nearby MLP situation. Moreover, the calculation time of the proposed method is obviously less than LASA and FSA for larger scale power system. The total computation time for the most effective preventive control variables selection can be reduced while remaining the good accuracy and robustness. In summary, the proposed method would be more suitable for an online application than the existing methods, especially for the large-scale power system.

### REFERENCES

- [1] K. T. Vu, C. C. Liu, C. W. Taylor, and K. M. Jimma, "Voltage instability: Mechanisms and control strategies," *Proceedings of the IEEE*, vol. 83, no. 11, pp. 1442–1455, Nov. 1995.
- [2] T. V. Cutsem, "Voltage instability: phenomena, countermeasures, and analysis methods," *Proceedings of the IEEE*, vol. 88, no. 2, pp. 208–227, 2000.
- [3] H. Liu, X. Chen, K. Yu and Y. Hou, "The Control and Analysis of Self-Healing Urban Power Grid," *IEEE Transactions on Smart Grid*, vol. 3, no. 3, pp. 1119–1129, Sept. 2012.
- [4] J. Y. Wen, Q. H. Wu, D. R. Turner, S. J. Cheng and J. Fitch, "Optimal coordinated voltage control for power system voltage stability," *IEEE Transactions on Power Systems*, vol. 19, no. 2, pp. 1115–1122, May 2004.

- [5] D. Karlsson; M. Hemmingsson and S. Lindahl, "Wide area system monitoring and control-terminology, phenomena, and solution implementation strategies," *IEEE Power and Energy Magazine*, vol. 2, no. 5, pp. 68-76, Sept.-Oct. 2004
- [6] W. M. Lin, W. C. Hung, C. H. Huang and K. H. Lu, "A preventive control for contingencies security," *2009 International Conference on Power Electronics and Drive Systems (PEDS)*, Taipei, 2009, pp. 252-256.
- [7] X. Wang, G. C. Ejebe, J. Tong and J. G. Waight, "Preventive/corrective control for voltage stability using direct interior point method," *IEEE Transactions on Power Systems*, vol. 13, no. 3, pp. 878-883, Aug 1998.
- [8] Zhihong Feng, V. Ajarapu and D. J. Maratukulam, "A comprehensive approach for preventive and corrective control to mitigate voltage collapse," *IEEE Transactions on Power Systems*, vol. 15, no. 2, pp. 791-797, May 2000.
- [9] F. Capitanescu, T. V. Cutsem, "Preventive control of voltage security: A multi-contingency sensitivity-based approach," *IEEE Transactions on Power Systems*, vol.17, no.2, pp:358-364, 2002.
- [10] . Milano, A. J. Conejo and R. Zarate-Minano. "General sensitivity formulas for maximum loading conditions in power systems", *IET Generation Transmission & Distribution*, Vol.1, no.3, pp.516-528, 2007.
- [11] G. Cai, Y. Zhang, R. Chen, and Z. Cai, "A fast corrective load shedding control scheme to prevent AC/DC systems voltage collapse", *European Transactions on Electrical Power*, vol.19, no.6, pp: 869-879, 2009.
- [12] S. Li, Y. Li, Y. Cao, Y. Tan, L. Jiang and B. Keune, "Comprehensive decision-making method considering voltage risk for preventive and corrective control of power system," *IET Generation, Transmission & Distribution*, vol. 10, no. 7, pp. 1544-1552, 5 5 2016.
- [13] S. Greene, I. Dobson, F. L. Alvarado, "Sensitivity of the loading margin to voltage collapse with respect to arbitrary parameters," *IEEE Transactions on Power Systems*, vol.12, no.1, pp: 262-272, 1997.
- [14] A. Venikov, V.A. Stroeve, V.I. Idelchick, and V.I. Tarasov, "Estimation of electric power system steady state stability in load flow calculations," *IEEE Transactions on PAS*, vol. PAS-94, No.3, pp. 1034-041, May 1975.
- [15] V. Ajarapu and C. Christy, "The continuation power flow: a tool for steady state voltage stability analysis," *IEEE Transactions on Power Systems*, vol. 7, no. 1, pp. 416-423, Feb 1992.
- [16] V. Ajarapu and C. Christy, "The continuation power flow: a tool for steady state voltage stability analysis," *IEEE Transactions on Power Systems*, vol. 7, no. 1, pp. 416-423, Feb 1992.
- [17] H. Khoshkhoo and S. M. Shahrtash, "Fast online dynamic voltage instability prediction and voltage stability classification," *IET Generation, Transmission & Distribution*, vol. 8, no. 5, pp. 957-965, May 2014.
- [18] M. R Mansour, M.; E.L Gerdali.; L.F.C Alberto, Andrade Ramos, R., "A New and Fast Method for Preventive Control Selection in Voltage Stability Analysis," *IEEE Transactions on Power Systems*, vol.28, no.4, pp.4448-4455, Nov. 2013
- [19] M. R. Mansour, L. F. C. Alberto and R. A. Ramos, "Preventive Control Design for Voltage Stability Considering Multiple Critical Contingencies," *IEEE Transactions on Power Systems*, vol. 31, no. 2, pp. 1517-1525, March 2016.
- [20] Y.H. Hong, C.T Pan, and W.W Lin, "Fast calculation of voltage stability index," *IEEE Transactions on Power Systems*, vol. 12, No. 4, November 1997.
- [21] L.D. Arya, S.C Choube, and M. Shrivastava, "Technique for voltage stability assessment using newly developed line voltage stability index," *Energy Conversion and Management*, vol.49, pp. 267-275, 2008.
- [22] K. Vu, M.M. Begovic, D. Novosel, M.M. Saha, "Use of local measurements to estimate voltage-stability margin," *IEEE Transactions on Power Systems*, vol.14, no.3, pp.1029-1035, Aug 1999
- [23] M.H. Haque, "On-line monitoring of maximum permissible loading of a power system within voltage stability limits," *IEE Proceedings Generation, Transmission and Distribution*, vol.150, no.1, pp.107-112, Jan. 2003
- [24] B. Milosevic, M. Begovic, "Voltage-stability protection and control using a wide-area network of phasor measurements," *IEEE Transactions on Power Systems*, vol.18, no.1, pp.121-127, Feb. 2003
- [25] F.A. Althowibi and M.W. Mustafa, "Voltage stability calculations in power transmission lines: Indications and allocations," *2010 IEEE International Conference on Power and Energy (PECon)*, vol., no., pp.390-395, Nov. 29 2010-Dec. 1 2010
- [26] G. Liu, H. Shi, Y. Yang, "Comprehensive Dynamic Analysis Method for Power System Static Voltage Stability," *Proceeding of the CSEE*, Vol.33, no.10, pp: 50-56, 2013.
- [27] Fuwen Yang, Zidong Wang and Y. S. Hung, "Robust Kalman filtering for discrete time-varying uncertain systems with multiplicative noises," *IEEE Transactions on Automatic Control*, vol. 47, no. 7, pp. 1179-1183, Jul 2002.
- [28] A. H. Sayed, "A framework for state-space estimation with uncertain models," *IEEE Transactions on Automatic Control*, vol. 46, no. 7, pp. 998-1013, Jul 2001.
- [29] R. Leelaruij, L. Vanfretti and M. S. Almas, "Voltage stability monitoring using sensitivities computed from synchronized phasor measurement data," *2012 IEEE Power and Energy Society General Meeting*, San Diego, CA, 2012, pp. 1-8.
- [30] IEEE 39-Bus System Description. [Online]. Available: <http://icseg.iti.illinois.edu/ieee-39-bus-system/>